

VFV as a New Effective CYP51 Structure-Derived Drug Candidate for Chagas Disease and Visceral Leishmaniasis

Galina I. Lepesheva,^{1,2} Tatiana Y. Hargrove,¹ Girish Rachakonda,³ Zdzislaw Wawrzak,⁴ Sébastien Pomel,⁵ Sandrine Cojean,⁵ Pius N. Nde,³ W. David Nes,⁶ Charles W. Locuson,⁷ M. Wade Calcutt,¹ Michael R. Waterman,¹ J. Scott Daniels,⁷ Philippe M. Loiseau,⁵ and Fernando Villalta³

¹Department of Biochemistry School of Medicine, ²Center for Structural Biology, Vanderbilt University, and ³Department of Microbiology and Immunology, Meharry Medical College, Nashville, Tennessee; ⁴Synchrotron Research Center, Life Science Collaborative Access Team, Northwestern University, Argonne, Illinois; ⁵Antiparasitic Chemotherapy, UMR 8076 CNRS BioCIS, University Paris-Sud, Chatenay-Malabry, France; ⁶Department of Chemistry and Biochemistry, Center for Chemical Biology, Texas Tech University, Lubbock; and ⁷Department of Pharmacology, Vanderbilt University Medical Center, Nashville, Tennessee

Sterol 14 α -demethylases (CYP51) are the enzymes essential for sterol biosynthesis. They serve as clinical targets for antifungal azoles and are considered as targets for treatment of human *Trypanosomatidae* infections. Recently, we have shown that VNI, a potent and selective inhibitor of trypanosomal CYP51 that we identified and structurally characterized in complex with the enzyme, can cure the acute and chronic forms of Chagas disease. The purpose of this work was to apply the CYP51 structure/function for further development of the VNI scaffold. As anticipated, VFV (R)-N-(1-(3,4'-difluorobiphenyl-4-yl)-2-(1H-imidazol-1-yl)ethyl)-4-(5-phenyl-1,3,4-oxadiazol-2-yl)benzamide, the derivative designed to fill the deepest portion of the CYP51 substrate-binding cavity, reveals a broader antiprotozoan spectrum of action. It has stronger antiparasitic activity in cellular experiments, cures the experimental Chagas disease with 100% efficacy, and suppresses visceral leishmaniasis by 89% (vs 60% for VNI). Oral bioavailability, low off-target activity, favorable pharmacokinetics and tissue distribution characterize VFV as a promising new drug candidate.

Keywords. Chagas disease; *Trypanosoma cruzi*; visceral leishmaniasis; *Leishmania*; sterol biosynthesis; sterol 14 α -demethylase (CYP51); inhibition; VNI; VFV; structure-based drug design.

Human infections with *Trypanosomatidae* represent a severe global health problem [1, 2]. Currently, these protozoan parasites affect more than 20 million people, producing significant morbidity and mortality. About 30 species of *Leishmania* cause different types of leishmaniasis that range from cutaneous lesions to deadly visceral forms, in which parasites populate the liver, spleen, and bone marrow. *Leishmania* is transmitted by the sandfly (*Phlebotomine*); in humans, it replicates intracellularly within macrophages. More than 70

genetically diverse strains of *Trypanosoma cruzi* (<http://www.dbbm.fiocruz.br/TcruziDB/strain.html>) are transmitted by kissing bugs (*Triatomine*), causing Chagas disease. Depending on the *T. cruzi* strain, Chagas disease varies significantly in its progression, severity, chronic symptoms (cardiac vs gastrointestinal), and drug sensitivity [3]. Bloodstream forms of *T. cruzi* infect a variety of human tissues, where they transform into amastigotes and multiply intracellularly. Two species of *T. brucei* cause sleeping sickness. They are transmitted by the tsetse fly (*Glossina*); in humans, they remain extracellular, multiplying in the bloodstream and subsequently entering the central nervous system.

Among these pathogens, only *T. brucei* is mainly confined to Africa. *Leishmania*, which used to be more common in tropical and subtropical areas, is now broadening its frontiers worldwide as human immunodeficiency virus coinfections [4]. Chagas disease remains endemic in South America, and is now spreading all over the

Received 16 December 2014; accepted 8 April 2015; electronically published 15 April 2015.

Correspondence: Galina I. Lepesheva, PhD, Department of Biochemistry School of Medicine, Vanderbilt University, 622 RRB, 2200 Pierce Ave, Nashville, TN 37232 (galina.i.lepesheva@vanderbilt.edu).

The Journal of Infectious Diseases® 2015;212:1439–48

© The Author 2015. Published by Oxford University Press on behalf of the Infectious Diseases Society of America. All rights reserved. For Permissions, please e-mail: journals.permissions@oup.com.

DOI: 10.1093/infdis/jiv228

globe, mainly due to human and vector migration. Currently, 2–7 million people infected with *T. cruzi* live in North America [5], and kissing bug bites are reported in 43 states in the United States. The treatment remains unsatisfactory: the existing drugs (benznidazole and nifurtimox for Chagas disease; pentavalent antimonials, amphotericin B, or miltefosine for leishmaniasis) have limited efficacy, and are highly toxic, the severe adverse side effects often leading to treatment discontinuation [2].

In 2012, two antifungal triazoles, posaconazole and ravuconazole, inhibitors of fungal sterol biosynthesis, entered clinical trials for Chagas disease. The results, unfortunately, were disappointing, and 70–80% treatment failure was reported [6, 7]. Further trials using longer treatment periods, higher drug doses, or combination therapy are expected. However, repurposing these drugs for treatment of protozoan infections has some limitations. Posaconazole is too expensive [8] to be used in endemic areas [6], and ravuconazole appears to have issues with bioavailability. Perhaps most importantly, both these 1,2,4-triazoles are inhibitors of fungal sterol 14 α -demethylases (CYP51), which have only 20–25% amino acid sequence identity to CYP51s in *Trypanosomatidae* [9].

In fungi, CYP51s (reviewed in [10]) catalyze the removal of the 14 α -methyl group from the cyclized ergosterol precursors: eburicol and/or lanosterol. Ergosterol is required for the formation of viable membranes (bulk role) and for different regulatory processes essential for cell growth and division (metabolic role) [11]. Similar to fungi, *Trypanosomatidae* also produce ergosterol and ergosterol-like molecules. However, indispensability of the endogenous bulk sterols is well established only for *T. cruzi* [12]. The situation with *Leishmania* remains unclear, and the bloodstream (human) forms of *T. brucei* can scavenge host cholesterol for their membranes [13], although they still express the CYP51 gene, and CYP51 inhibition slows down the development of parasitemia in a mouse model of sleeping sickness [14], thus implying that they must require endogenous regulatory sterols.

Recently, we have shown that VNI, (R)-N-(1-(2,4-dichlorophenyl)-2-(1H-imidazol-1-yl)ethyl)-4-(5-phenyl-1,3,4-oxadiazol-2-yl)benzamide, a potent experimental inhibitor of Tulahuen strain *T. cruzi* CYP51, can cure with 100% efficiency the acute and chronic Chagas disease in mice [15]. Here we compare antiprotozoan activity of VNI with its derivative VFV, (R)-N-(1-(3,4'-difluorobiphenyl-4-yl)-2-(1H-imidazol-1-yl)ethyl)-4-(5-phenyl-1,3,4-oxadiazol-2-yl)benzamide that was CYP51 structure-based designed with the goal to further strengthen its inhibitory potency and broaden the antiparasitic spectrum of action.

METHODS

Animal Studies

Animal studies on pharmacokinetics and the mouse model of Chagas disease were conducted under the National Institutes of Health (NIH) guidelines on the humane use and care of

laboratory animals for biomedical research (NIH Publication No. 85–23). Protocols were approved by the Meharry Medical College Institutional Animal Care and Use Committee. Animal studies on leishmaniasis were performed under the French guidelines on care of laboratory animals. The animal house facility has the French agreement #A92-019-01 and conforms to the French ethics rules concerning animal experimentations.

VNI Derivatives and Enzymatic and Crystallographic Analysis of CYP51 Inhibition

CYP51 inhibitors, PDB IDs VNI, VNF, VNT, and VFV, were synthesized at the Vanderbilt Chemical Synthesis Core. The CYP51 enzymes were purified and assayed as described previously [16, 17]. The VFV and VNT costructures (2.05 and 1.82Å resolution, respectively) were determined by molecular replacement using ligand-free *T. brucei* CYP51 (PDB ID 3G1Q) as a template. [Supplementary Table 1](#) summarizes the diffraction and refinement statistics. Structure superimposition was performed in LSQkab (CCP4 Program Suite) using a secondary structure matching algorithm.

Cellular Infection Assay

The efficacies of VNI derivatives in cellular experiments with *T. cruzi* were evaluated using the same experimental conditions and the green fluorescent protein-expressing trypomastigote clone 20A [18] of Tulahuen *T. cruzi* that we used previously to compare the activities of VNI, posaconazole, and ravuconazole [15]. Antileishmanial effects of the compounds were examined on axenic and intramacrophagic amastigotes of *Leishmania donovani* as described previously [19].

Pharmacokinetics, Metabolism and Tissue Distribution in Mice

The pharmacokinetics and tissue distribution were studied using the protocol based on the VNI-specific absorption maximum at 291 nm [15]. In all in vivo experiments, fresh solutions of the compounds (5% stocks in dimethyl sulfoxide dissolved in sterile 5% Arabic gum in phosphate-buffered saline containing 0.5% Tween 80) were given to BALB/c mice (Jackson Laboratory) at 25 mg/kg by oral gavage. To obtain a single-dose profile, the blood samples were collected over time. To monitor drug concentration after multiple doses, VNI or VFV were administered twice a day for 5 days (20 mice per group). Four hours after the first administration and then every 12 hours, 2 mice from each group were sacrificed; their blood, hearts, lungs, skeletal muscle, liver, and spleen were collected. The compounds were extracted from plasma as described for VNI [15]. To analyze their tissue distribution, prior to drug extraction approximately 100 mg of each tissue was diluted 5-fold with water and homogenized. VNI and VFV metabolites [M + 34] were characterized by liquid chromatography high-resolution mass spectrometry. The details are provided in the legend to [Supplementary Figure 1](#).

Hepatic Microsomal Stability and Human Cytochrome P450 Inhibition Assays

Hepatic stability of VNI and VFV were assayed in mouse, rat, and human microsomes (BD Biosciences San Jose, California) following the manufacturer's instructions. The drugs were quantified using a Thermo TSQ mass spectrometer (Waltham, Massachusetts) coupled to a LC-20AD Shimadzu high-performance liquid chromatography system (Columbia, Maryland) with Fortis C18 column (2.1 × 50 mm, 3 μm). The scaled CL_{int} (mL/min/kg) and CL_{hep} (mL/min/kg) were calculated as described [20]. Inhibition of human CYP1A2, 2C9, and 2D6 was conducted in liver microsomes using a cocktail of substrates at their K_m values (40 μM phenacetin, 5 μM diclofenac, and 5 μM dextromethorphan, respectively) [21].

VFV Efficacy Studies in an Animal Model of Chagas Disease

The experiments were conducted as previously described for VNI [15]. At these conditions, parasitemia reaches its maximum 14 days after infection, causing death in 100% of untreated animals [22]. Animals reaching the peak of parasitemia were euthanized. After 30 days of VFV treatment, the mice were immunosuppressed with cyclophosphamide (100 mg/kg) to reactivate infection. On day 62, the animals were euthanized. Blood, tissues, and organs were collected to determine the presence of *T. cruzi* by real-time-polymerase chain reaction (RT-PCR) analysis as described in [15]. Briefly, genomic DNA was purified from the organs, tissues, and blood using the DNeasy tissue and blood isolation kit (Qiagen, Valencia, California). Parasite genomic DNA was purified from epimastigotes. A standard curve in the range of 50 pg to 50 ng for the detection of *T. cruzi* DNA by RT-PCR (iCycler; Bio-Rad) was developed using the *T. cruzi* 195-base pair (bp) repeat DNA (GenBank accession no. AY520044)-specific primers TCZ1 5'-CGA GCT CTT GCC CAC ACG GGT GCT-3' and TCZ2 5'-CCT CCA AGC AGC GGA TAG TTC AGG-3', which amplify a *T. cruzi* 188-bp

sequence. The negative cycle threshold values were established in the control experiments using organs, tissues, and blood of mice that were not infected with *T. cruzi*.

VNI and VFV Efficacy in an Animal Model of Visceral Leishmaniasis

The experiments were performed following the previously described basic protocol [23] with minor modifications. Mice (Elvages Janvier, France) were infected intravenously with 10^7 *L. donovani* amastigotes derived from an infected golden hamster spleen. Treatment with VFV and VNI was started 1 week after infection and lasted for 10 or 20 consecutive days. Liposomal amphotericin B (AmBisome) was used as reference treatment. Two days after treatment, the animals were sacrificed, and livers and spleens were weighed. Smears were alcohol-fixed, stained, and examined under a light microscope. Parasite load in the organs was determined microscopically by counting the number of parasites/1000 liver cells in Giemsa-stained impression smears prepared from the liver. The *U*-rank test was used for statistical analysis.

Analysis of Leishmania Sterols

Promastigotes of *L. amazonensis* (1×10^{10} parasites) were grown in M199 medium supplemented with 10% heat-inactivated fetal bovine serum without inhibitor (control) or in the presence of 1 μM VNI for 3 days at 25°C. Sterols were extracted and analyzed as described previously [16]; more details are provided in [Supplementary Table 2](#).

RESULTS AND DISCUSSION

Inhibition of Protozoan CYP51s and Crystallographic Analysis of Structure-Activity Relationship

VNI and VNF (Figure 1) were both identified as highly potent inhibitors of trypanosomal sterol 14α-demethylases in the

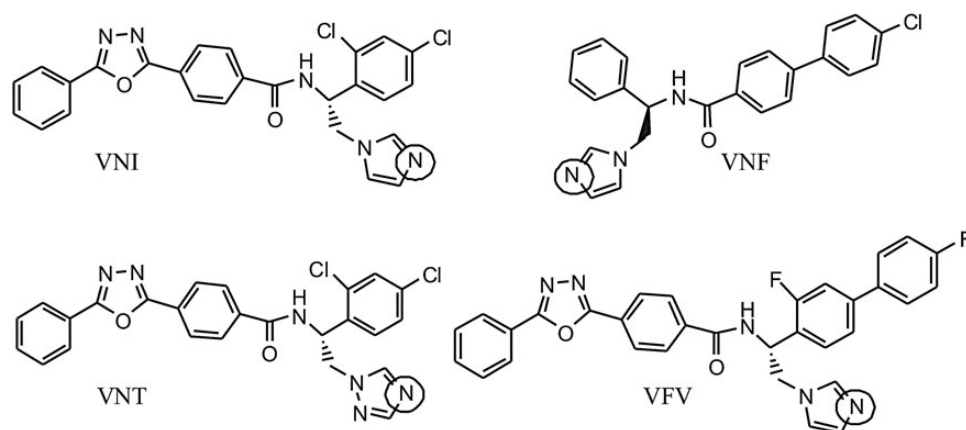


Figure 1. Chemical structures of VNI, VNF, VNT, and VFV. The basic Fe-coordinating nitrogen atoms are circled. VNI, VNF, VNT, and VFV are the compounds PDB IDs, their IUPAC names being as follows: VNI, (R)-N-(1-(2,4-dichlorophenyl)-2-(1H-imidazol-1-yl)ethyl)-4-(5-phenyl-1,3,4-oxadiazol-2-yl)benzamide; VNF, (R)-N-(2-(1H-imidazol-1-yl)-1-phenylethyl)-4'-chlorobiphenyl-4-carboxamide; VNT, (R)-N-(1-(2,4-dichlorophenyl)-2-(1H-1,2,4-triazol-1-yl)ethyl)-4-(5-phenyl-1,3,4-oxadiazol-2-yl)benzamide; VFV, (R)-N-(1-(3,4'-difluorobiphenyl-4-yl)-2-(1H-imidazol-1-yl)ethyl)-4-(5-phenyl-1,3,4-oxadiazol-2-yl)benzamide.

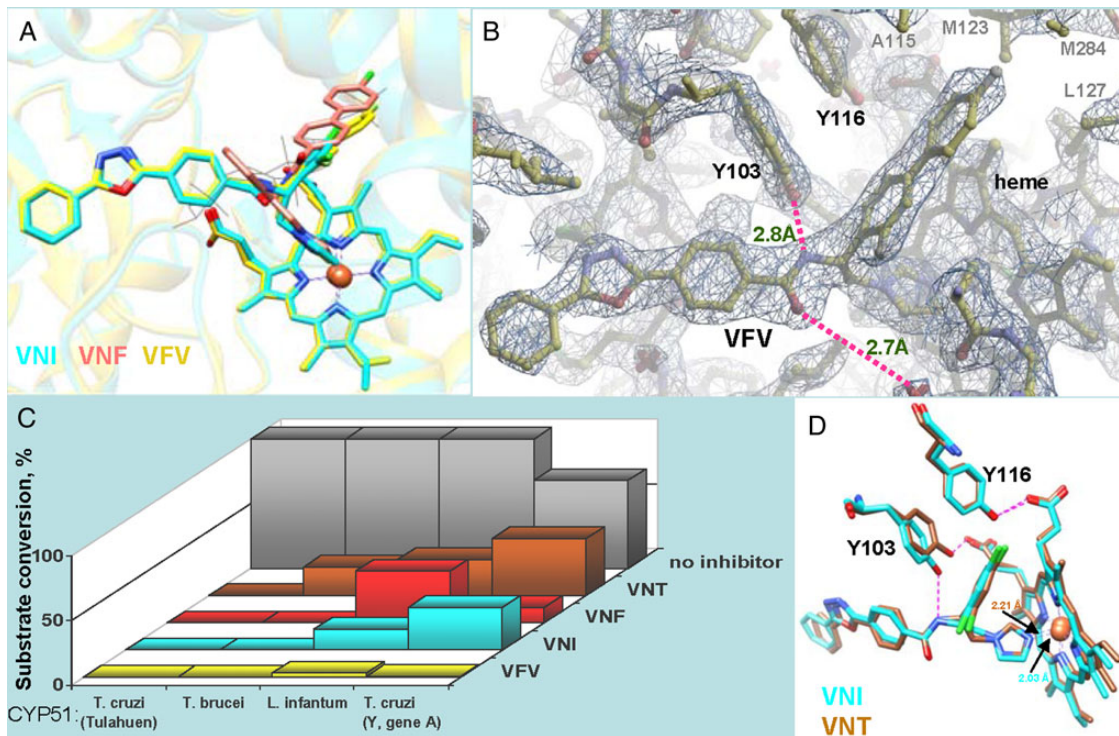


Figure 2. Structural basis for the broader antiprotozoan spectrum of action of VFV. *A*, Binding modes of VNI (cyan), VNF (salmon), and VFV (yellow) in the superimposed CYP51 costructures (PDB ID 3GW9, 3KSW, and 4G7G, respectively). The secondary structural elements of the protein are seen as semi-transparent ribbons of the corresponding colors. A molecule of the CYP51 substrate eburicol is delineated in gray lines as a reference. *B*, 2Fo-Fc electron density map (1.5 σ) of the VFV-bound area in the CYP51 costructure (PDB ID 4G7G). The H-bond network is shown in purple, the distances are marked. *C*, Inhibitory effects of VNI, VNF, VNT, and VFV on sterol 14 α -demethylase activity of 4 protozoan CYP51 orthologs at 1/1/50 molar ratio inhibitor/enzyme/substrate [16, 17]. P450 concentration 0.5 μ M; 1-hour reaction. *T. brucei* cytochrome P450 reductase [27] was used as the electron donor. While all the derivatives are potent inhibitors of Tulahuen *T. cruzi* CYP51, only VFV reveals about the same strong potency against different tested protozoan CYP51 orthologs, including *L. infantum* and *Y-T. cruzi* CYP51A (*Y* strain *T. cruzi* has 2 CYP51 genes, gene A was shown to be resistant to inhibition [28]). *D*, In 1 of the 4 *T. brucei* CYP51-VNT molecules (4G3J, brown), the side chain of Y103 remains in contact with the heme propionate, and the H-bond network with the inhibitor is not formed, which is in good agreement with the weaker inhibitory effect of VNT on *T. brucei* CYP51 activity (shown in panel *C*). Superimposition with VNI in 3GW9, cyan. The Fe-N coordination bonds are 2.21 Å and 2.03 Å , respectively.

reconstituted CYP51 reactions [16] and subsequently cocrystallized with the *T. brucei* [14] and *T. cruzi* [24] CYP51 orthologs. As expected, in the enzyme active site they both coordinate to the heme iron via the N3-imidazole nitrogen. The other 2 structural modules of their molecules, however, adopt opposite orientations. While the 3-ring arm of VNI occupies the substrate access channel, the 2-ring arm of VNF is projected toward the deepest, CYP51-specific [25] portion of the binding cavity that physiologically accommodates the aliphatic arm of the sterol substrate [26]. Interestingly, the carboxamide fragment of VNI appeared to play an important role by forming a hydrogen bond network with the protein [14], thus enhancing the binding (the energy of an H-bond is 5–50-fold higher than the energy of van der Waals interactions) and assuring high antiprotozoan selectivity [2]. VFV was designed as the VNI/VNF hybrid molecule (Figure 2A) with the goal to further strengthen the drug inhibitory potency by filling the deepest portion of the CYP51-binding cavity and thus generating additional protein–ligand interactions. Indeed, while

VNI forms van der Waals contacts (<4.5 Å) with 16 CYP51 amino acids, VFV interacts with 22. Four of the 6 additional VFV-contacting residues are seen in Figure 2B, marked in gray. VNT, the VNI 1,2,4-triazole derivative, was conceived to test whether it may reveal a higher selectivity as a CYP51 inhibitor (which has been confirmed and is shown in Figure 2C) due to the lower basicity of its N4-nitrogen and potentially a weaker Fe-N coordination bond [21] (shown in Figure 2D). Another reason for the VNT design was to explore a possibility of its longer lifetime in plasma [29, 30].

Antiparasitic Effects in Tulahuen *T. cruzi* Amastigotes

In accordance with their high potency to inhibit Tulahuen *T. cruzi* CYP51, all 4 compounds displayed remarkable intracellular antiparasitic activity (Figure 3), clearing Tulahuen *T. cruzi* infection in vitro at low nanomolar concentrations. Of them, the lowest median effective concentration (EC₅₀) values, 0.8 and 1.0 nM, were achieved in the presence of VFV and VNT, respectively,

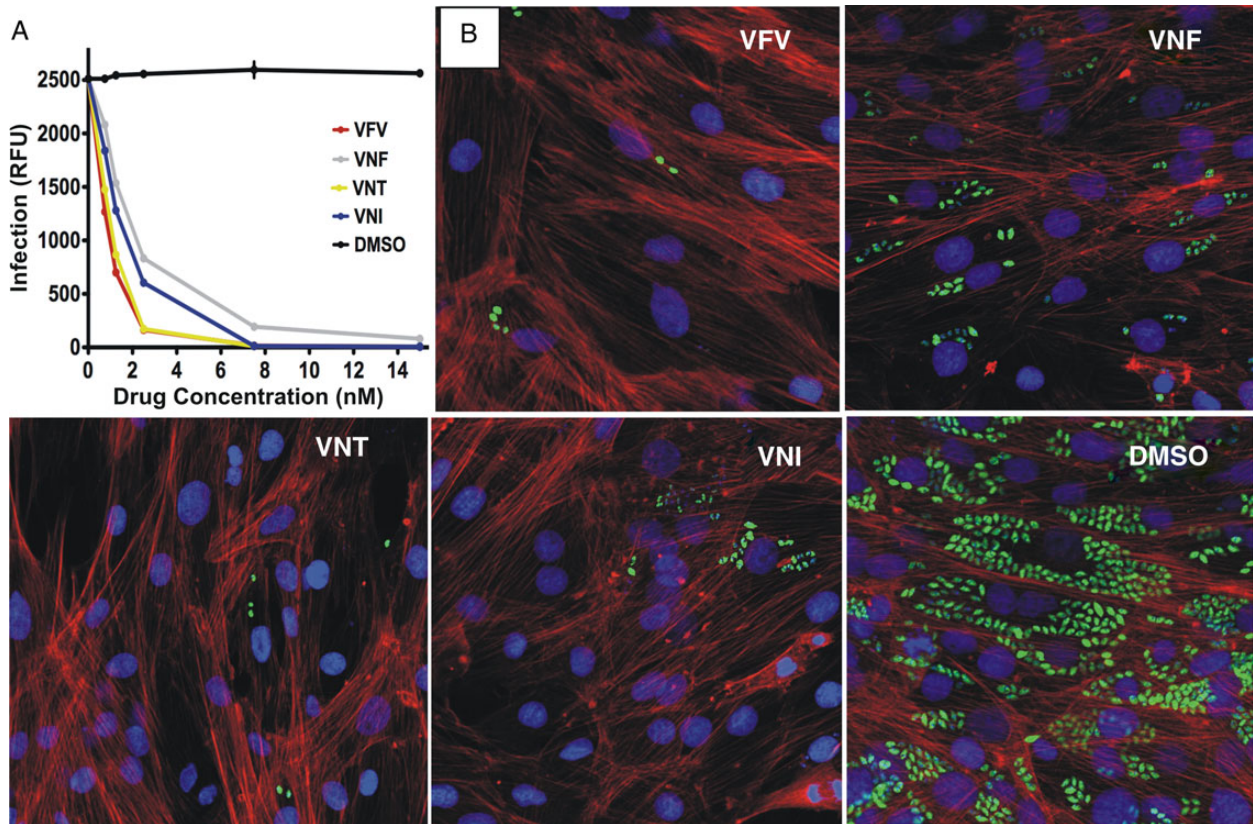


Figure 3. Cellular effects of CYP51 inhibitors in Tulahuen *T. cruzi* infected cardiomyocytes. *A*, Comparative dose-dependent clearance of the parasite. Cardiomyocyte monolayers were exposed to green fluorescent protein-expressing Tulahuen trypomastigotes (10 parasites per cell) for 24 hours and then treated with 1–16 nM VNI, VNF, VFV, VNT, or DMSO. The infection was quantified by determining the fluorescence level of parasites expressing green fluorescent protein, indicated as relative fluorescence units (RFUs) 72 hours after infection. Data represent the mean values \pm SEM of the results from triplicate samples. *B*, Fluorescence microscopic observations of Tulahuen *T. cruzi* inside cardiomyocytes treated with 4 nM of VNI, VNF, VFV, VNT, or DMSO 72 hours after infection. The monolayers were fixed with 2.5% paraformaldehyde and stained with 4',6-diamidino-2-phenylindole to visualize DNA, and with Alexa fluor to visualize actin myofibrils. *Trypanosoma cruzi* amastigotes are green, cardiomyocyte nuclei are blue, and cardiomyocyte actin myofibrils are red. Abbreviations: DMSO, dimethyl sulfoxide; SEM, standard error of the mean.

which may be related, at least in part, to their higher lipophilicity (logP) and therefore better cellular permeability. The complete clearance of the parasite infection in cardiomyocytes was observed at <8 nM concentrations of VNI, VNT, and VFV, whereas some amastigotes were still detected at up to 15 nM VNF, which therefore was not included into further experiments.

Pharmacokinetics, Tissue Distribution and Biotransformation

When administered as a single oral dose, VNI, VFV, and VNT displayed quite different results (Figure 4A). Although the time-concentration curves for VNI and VFV are comparable in shape, the peak plasma level of VNI is higher (approximately 40 μ M vs approximately 25 μ M for VFV), but the slope of its curve is sharper. As a result, no trace of VNI is present in plasma 18 hours after administration, while VFV can still be detected after 26 hours. The triazole VNT is also seen in plasma for at least 26 hours, thus indeed displaying a longer lifetime. Yet, its concentration remains <3.5 μ M, indicating drastically lower bioavailability.

Because oral bioavailability is crucial for potential antitrypanosomatid agents [6], as well as because VNT turned out to be too selective, only VNI and VFV were tested in further studies.

After multiple oral doses, VNI and VFV plasma concentrations remain rather stable (Figure 4B), which is in agreement with their favorable in vivo safety profiles [31]. Formation of a more polar metabolite was observed in both cases (Figure 4C), the rate being higher for VFV. Mass spectrometric analysis (Supplementary Figure 1) showed that each metabolite has the molecular weight [M + 34] (538.1043 and 582.1943, for VNI (504.0989) and VFV (548.1894), respectively), their fragmentation patterns indicating addition of 2 OH-groups to the imidazole ring, the process that has been reported for other imidazoles as well [32]. The site and type of biotransformation pointed out that VNI and VFV conversion is likely to occur in the liver. This was confirmed in human, rat, and mouse liver microsomes, where an allometric relationship across species was observed (Table 1), and the same [M + 34] metabolites

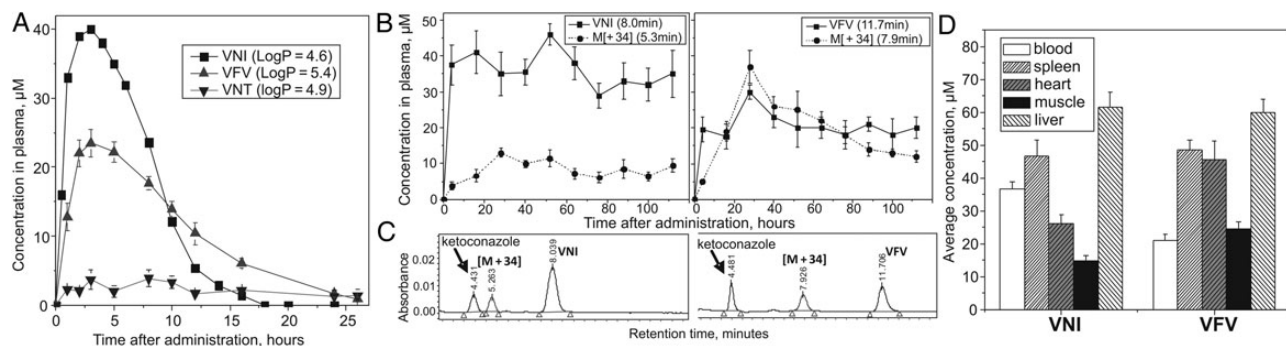


Figure 4. Pharmacokinetics and tissue distribution. The analysis was performed using reverse-phase high-performance liquid chromatography (HPLC). The HPLC system was equipped with the dual-wavelength UV 2489 detector (Waters) set at 291 and 250 nm and Symmetry C18 (3.5 μ m) 4.6 \times 75 mm column. The mobile phase was 55% 0.01 M ammonium acetate (pH 7.4) and 45% acetonitrile (v/v) with an isocratic flow rate of 1.0 mL/min. *A*, Single oral dosage profiles of VNI, VFV, and VNT. The compounds were administered by oral gavage at 25 mg/kg. *B*, Detection of VNI, VFV, and their metabolites [M + 34] in plasma after multiple oral doses (25 mg/kg twice a day for 5 days). *C*, Examples of HPLC profiles (112-hour samples), the UV detector was set at 291 nm, and 50 μ M ketoconazole was used as an internal standard. *D*, VNI and VFV tissue distribution after multiple oral doses. The bars represent average drug concentration (the mean values \pm SEM) within the time period of 16–112 hours. Abbreviations: SEM, standard error of the mean; UV, ultraviolet.

were identified (not shown). Thus, although the imidazole ring was reported as a potentially metabolically vulnerable portion of this class of drugs (eg, at a single dose of 60 mg/kg, the lifetime of ketoconazole in mouse plasma is only 7 hours [33]), our experiments support the notion [29] that the metabolic stability of imidazoles may vary substantially depending on the compound composition. Because both metabolites are formed as a result of hydroxylation of the heme-coordinating ring of the parent drugs, we evaluated the inhibitory effects of VNI and VFV on the major human drug-metabolizing P450s. Both compounds demonstrated weak P450 inhibition (Table 1), though the data may suggest some involvement of CYP1A2, because this is the only CYP that is more strongly affected by VFV. Further experiments are needed to establish the detailed biotransformation process, yet it appears to differ from that of the clinical antifungals posaconazole, itraconazole, or ketoconazole, which are known to be strong inhibitors and substrates of CYP3A4 [29, 34]. In general, VNI and VFV show low and moderate hepatic clearance, respectively, and weak influence on the major drug-metabolizing CYPs, which are good characteristics of potential human drugs.

VNI and VFV also revealed a very favorable tissue distribution (Figure 4D). Interestingly, the concentration of VFV in tissues is higher than in the blood, particularly in the heart and muscle, where it also significantly exceeds the concentration of VNI. Altogether, the data analysis makes it reasonable to believe that the lower concentration of VFV in blood may be due to combination of its faster blood clearance and stronger affinity to tissues/organs. Stronger affinity of VFV to tissues/organs may be a result of its higher lipophilicity, while its relatively longer lifetime in plasma after a single oral dose can reflect a slower rate of absorption, which in turn may imply higher VFV concentrations in the gastrointestinal tract. All these features can be of special value in targeting intracellular pathogens, such as *T. cruzi*, which mainly inhabit the heart, skeletal muscles, and the gut, the latter being suggested as the site where quiescent forms of *T. cruzi* congregate to evade host immune-defense mechanisms [35]. Further work on VFV metabolic stabilization might be advantageous and is currently in progress, but overall its drug-like properties were found quite satisfactory to proceed to in vivo experiments.

Table 1. Clearance of VNI and VFV in Human, Rat, and Mouse Microsomes and Their Inhibitory Effects (IC₅₀) on the Activity of Major Human Drug-Metabolizing CYPs

Compound	Human			Rat			Mouse			IC ₅₀ , μ M			
	t _{1/2} (min)	CL _{INT} ^a	GL _{HEP}	t _{1/2} (min)	CL _{INT}	GL _{HEP}	t _{1/2} (min)	CL _{INT}	GL _{HEP}	1A2	2C9	2D6	3A4 ^b
VNI	>60	4.38	3.62	31	90.6	39.5	31	178	59.8	5.61	2.06	1.63	0.4
VFV	50	24.5	11.3	41	69.0	34.8	18	313	69.9	0.82	4.40	1.46	3.6

Abbreviation: IC₅₀, median inhibitory concentration.

^a The values used for mouse liver weight (g): body weight (kg) and the hepatic flow were 87.5 and 90 (mL/min/kg), respectively.

^b The IC₅₀ values for CYP3A4 were determined previously [15, 31].

Curative Effect of VFV in a Mouse Model of the Acute Chagas Disease

Because it is quite well known that high antiparasitic potency of a compound in cellular experiments does not necessarily indicate its activity in vivo [7, 12, 33], it was important to verify the ability of VFV to cure Chagas disease in animal models. Infection of mice with *T. cruzi* and treatment with VFV were performed following the scheme previously used for treatment with VNI [15]. Results in Figure 5 show that parasitological clearance and survival rate were 100%. No side effects were noticed: the mice had normal appearance during the whole treatment period and there was an increase in their body weight, occurring at the same rate as in the uninfected group of animals. No relapse of parasitemia was observed after 6 rounds of post-treatment immunosuppression. RT-PCR analysis confirmed 100% parasitological cure in all tested tissues, organs, and blood of all treated animals. Taking into account that the CY-treated mice were challenged with a lethal dose of *T. cruzi*, the results are remarkable and clearly indicate that VFV is a new drug candidate that is highly potent and effective in vivo.

Comparative Effects of VNI and VFV in a Mouse Model of Visceral Leishmaniasis

Although endogenously produced sterols are required for cell proliferation and viability of parasites of the genus *Leishmania* [36, 37], the information about the use of antifungal azoles for anti-

leishmanial chemotherapy remains controversial, often depending on *Leishmania* species and the type of infection [38–43]. Visceral leishmaniasis, which is caused by *L. donovani* complex (*L. donovani*, *L. infantum*, and *L. chagasi*) and represents the most severe form of the disease, was reported to be the least sensitive [44].

Before proceeding to in vivo studies, antileishmanial activities of VNI and VFV were tested in cellular experiments against axenic and intramacrophage amastigotes of *L. donovani* and found comparable to that of the reference drugs miltefosine and AmBisome (Table 2). In the in vivo experiments, mice infected with *L. donovani* were treated with VNI and VFV, using the same dosage and administration route as described above for *T. cruzi*. AmBisome was administered 3 times at a higher dose (1 mg/kg) or 10 times at a lower dose (0.2 mg/kg), which is considered the optimal use of AmBisome in experimental models of leishmaniasis because of its toxicity. The 20-day treatment with VNI and VFV resulted in 60% (VNI) and 89% (VFV) reduction of parasitemia, all animals survived, and no side effects were observed (Table 2). Though, unlike in the Chagas disease model, the effects achieved at these conditions were only suppressive, the data demonstrate that both compounds have in vivo activity against visceral leishmaniasis and because of their low toxicity deserve further testing. Higher potency of VFV correlates well with its stronger inhibitory effect on the activity of the target enzyme (Figure 2C; *L. infantum* and *L. donovani* CYP51s have 100% amino acid sequence identity).

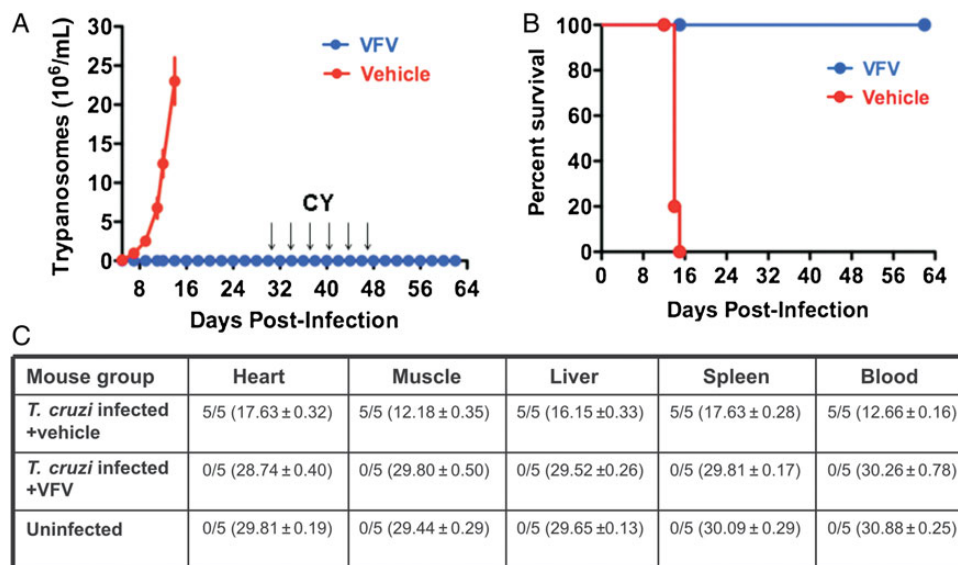


Figure 5. VFV cures *Trypanosoma cruzi* infection in vivo. *A*, Female BALB/c mice (5 per group) were intraperitoneally infected with a lethal dose of Tulahuen *T. cruzi* bloodstream trypomastigotes (1×10^5 organisms), followed by oral treatment with either VFV (25 mg/kg) or with drug vehicle twice per day for 30 days. Mice were then immunosuppressed by 6 injections of cyclophosphamide (CY, arrows). Three independent experiments were performed using the same protocol and provided similar results. Data represent the mean values \pm SEM. *B*, Kaplan–Meier survival plot. *C*, Results of RT-PCR for detection of *T. cruzi* in organs, tissues, and blood. Samples from each mouse group were tested in triplicate. The data in each column are the number of *T. cruzi*-positive mice/number in group (mean \pm standard error) cycle threshold for parasite detection. Abbreviations: RT-PCR, real-time–polymerase chain reaction; SEM, standard error of the mean.

Table 2. In Vitro and in Vivo Activity of VNI and VFV Against *Leishmania donovani*

Compound/ Formulation	In Vitro Activity		In Vivo Activity			Reduction of Parasitemia (%)
	EC ₅₀ (μM ± SD)		Regimen	Number of Mice	Route	
	Axenic Amastigotes	Intramacrophage Amastigotes				
VNI	2.29 ± 0.40	6.68 ± 0.97	25 mg/kg × 2/day × 20 d	10	p.o.	60 ^{a,b}
VFV	6.32 ± 0.91	0.42 ± 0.02	25 mg/kg × 2/day × 20 d	10	p.o.	89 ^{a,b}
			25 mg/kg/day × 10 d	10	p.o.	28
Miltefosine	5.2 ± 0.7	6.40 ± 0.75				
AmBisome	0.71 ± 0.2	1.14 ± 0.45	1 mg/kg at days 5, 7, 9	12	i.v.	93 ^a
			0.2 mg/kg/day × 10 d	12	i.v.	87 ^a
Control (vehicle)	0.2 mL × 2/day × 20 d	12	p.o.	0

Abbreviations: EC₅₀, median effective concentration; i.v., intravenously; p.o., by mouth.

^a Versus control mice; *P* < .05.

^b VFV versus VNI; *P* = .515.

In order to verify that the effects of VNI/VFV in *Leishmania* are due to alterations in the parasite sterols, we examined the sterol composition of *Leishmania* cells, untreated or treated with 1 μM VNI. The results show that contrary to fungi [45, 46] or *T. cruzi* [16], where CYP51 inhibition stops the pathway at the stage of lanosterol/eburicol, in *Leishmania* these C4-dimethylated sterols do not accumulate (Supplementary Table 2). Instead, they undergo further conversions, leading to the appearance of C4-desmethylated 14α-methylzymosterol and 14α-methylfecosterol. A relatively low (2-fold) decrease in the content of 5-dehydroepisterol and ergosterol may be due to some delay between CYP51 inhibition and exhaustion of the previously synthesized endogenous sterols. However, it cannot be excluded that 5-dehydroepisterol and ergosterol are still produced via 14α-demethylation of the C4-desmethyl sterols because of the higher substrate promiscuity of leishmanial CYP51 [17]. Branching of the sterol biosynthetic pathway may well be the cause for the weaker (slower) effect of CYP51 inhibitors in *Leishmania*, thus calling for drug combinations, particularly with sterol biosynthetic inhibitors that would work upstream the pathway (eg, an inhibitor of squalene epoxidase terbinafine [42] or azasterols, which inhibit sterol 24-methyl transferase [47]).

Concluding Remarks

For about 50 years, azoles have been used as antifungal agents in medicine, each new compound being discovered and developed empirically, by monitoring its action on fungal cell growth. Although it was proven by sterol analysis that azoles inhibit ergosterol biosynthesis in fungi by preventing sterol 14α-demethylation [48], the target CYP51 enzymes still remain excluded from the drug discovery process, mainly due to their highly hydrophobic membrane-bound nature, which complicates their handling and assay in vitro. Biochemical [16, 27, 49] and structural [14, 17, 24] characterization of protozoan CYP51s

opened new opportunities for target-driven drug discovery. Perfect superposition of VNI and VFV in the protozoan CYP51 active site confirms sterol 14α-demethylase as an excellent template for rational structure-based inhibitor design. The H-bond network found in the CYP51 costructures with all 3 VNI derivatives must be the basis for this scaffold antiprotozoan potency and selectivity. Deeper projection of the second aromatic ring into the CYP51 substrate-binding cavity makes VFV a more potent inhibitor for a broader variety of protozoan CYP51 orthologs. Good oral bioavailability, pharmacokinetics, and tissue distribution, as well as low off-target activity, characterize this new nontoxic and inexpensive compound as an attractive drug candidate. While it might benefit from further metabolic stabilization, its broader testing in vivo, preferably by a pharmaceutical company, would significantly impact the current treatment for Chagas disease, visceral leishmaniasis, and perhaps sleeping sickness as well, either as a monotherapy, or in combination with other antiprotozoan drugs. This would decrease their dosage and therefore alleviate the adverse toxic effects [50].

Supplementary Data

Supplementary materials are available at *The Journal of Infectious Diseases* online (<http://jid.oxfordjournals.org>). Supplementary materials consist of data provided by the author that are published to benefit the reader. The posted materials are not copyedited. The contents of all supplementary data are the sole responsibility of the authors. Questions or messages regarding errors should be addressed to the author. Supplementary data include the table summarizing the X-ray data collection and refinement statistics on the CYP51-VFV and CYP51-VNT costructures, the figure showing the results of VNI, VFV, and their [M + 34] metabolites mass spectrometric analysis, and the table comparing sterol composition of *Leishmania amazonensis* in the presence and absence of VNI.

Notes

Financial support. This work was supported by the National Institutes of Health GM067871, GM064841-S10 (G. I. L.), and in part by AI080580

and U54 MD007593 (F. V.), AI083925 (P. N. N.) and National Science Foundation MCB-0929212 (W. D. N.). The Confocal Microscopy Facility at Meharry was supported by G12 MD007586.

Potential conflicts of interest. All authors: No reported conflicts.

All authors have submitted the ICMJE Form for Disclosure of Potential Conflicts of Interest. Conflicts that the editors consider relevant to the content of the manuscript have been disclosed.

References

1. Research priorities for Chagas disease, human African trypanosomiasis and leishmaniasis. WHO Technical Report Series **2012**; 975.
2. Lepesheva GI, Waterman MR. Sterol 14 α -demethylase (CYP51) as a therapeutic target for human trypanosomiasis and leishmaniasis. *Curr Top Med Chem* **2011**; 11:2060–71.
3. Filardi LS, Brener Z. Susceptibility and natural resistance of *Trypanosoma cruzi* strains to drugs used clinically in Chagas disease. *Trans R Soc Trop Med Hyg* **1987**; 81:755–9.
4. van Griensven J, Carrillo E, López-Vélez R, Lynen L, Moreno J. Leishmaniasis in immunosuppressed individuals. *Clin Microbiol Infect* **2014**; 20:286–99.
5. Hotez P, Dumonteil E, Betancourt Cravioto M, Bottazzi M, Tapia-Conyer R. An unfolding tragedy of Chagas disease in North America. *PLOS Negl Trop Dis* **2013**; 7:e2300.
6. Molina I, Gómez i Prat J, Salvador F, et al. Randomized trial of posaconazole and benznidazole for chronic Chagas' disease. *N Engl J Med* **2014**; 370:1899–908.
7. Chatelain E. Chagas disease drug discovery: toward a new era. *J Biomol Screen* **2015**; 20:22–35.
8. Dobish MC, Villalta F, Waterman MR, Lepesheva GI, Johnston JN. Organocatalytic, enantioselective synthesis of VNI: a robust therapeutic development platform for Chagas, a neglected tropical disease. *Org Lett* **2012**; 14:6322–5.
9. Lepesheva GI, Villalta F, Waterman MR. Targeting *Trypanosoma cruzi* sterol 14 α -demethylase (CYP51). *Adv Parasitol* **2011**; 75:65–87.
10. Lepesheva GI, Waterman MR. Sterol 14 α -demethylase cytochrome P450 (CYP51), a P450 in all biological kingdoms. *Biochim Biophys Acta* **2007**; 1770:467–77.
11. Bloch KE. Sterol structure and membrane function. *CRC Crit Rev Biochem* **1983**; 14:47–92.
12. Urbina JA. Ergosterol biosynthesis and drug development for Chagas disease. *Mem Inst Oswaldo Cruz* **2009**; 104(suppl 1):311–8.
13. Coppens I, Courtroy PJ. The adaptative mechanisms of *Trypanosoma brucei* for sterol homeostasis in its different life-cycle environments. *Annu Rev Microbiol* **2000**; 54:129–56.
14. Lepesheva GI, Park HW, Hargrove TY, et al. Crystal structures of *Trypanosoma brucei* sterol 14 α -demethylase and implications for selective treatment of human infections. *J Biol Chem* **2010**; 285:1773–80.
15. Villalta F, Dobish MC, Nde PN, et al. VNI cures acute and chronic experimental Chagas disease. *J Infect Dis* **2013**; 208:504–11.
16. Lepesheva GI, Ott RD, Hargrove TY, et al. Sterol 14 α -demethylase as a potential target for antitrypanosomal therapy: Enzyme inhibition and parasite cell growth. *Chem Biol* **2007**; 14:1283–93.
17. Hargrove TY, Wawrzak Z, Liu J, Nes WD, Waterman MR, Lepesheva GI. Substrate preferences and catalytic parameters determined by structural characteristics of sterol 14 α -demethylase (CYP51) from *Leishmania infantum*. *J Biol Chem* **2011**; 286:26838–48.
18. Lima MF, Villalta F. *Trypanosoma cruzi* trypomastigote clones differentially express a parasite cell adhesion molecule. *Mol Biochem Parasitol* **1989**; 33:159–70.
19. Audisio D, Messaoudi S, Cojean S, et al. Synthesis and antikinoplastid activities of 3-substituted quinolinones derivatives. *Eur J Med Chem* **2012**; 52:44–50.
20. Obach RS. Prediction of Human Clearance of twenty-nine drugs from hepatic microsomal intrinsic clearance data: an examination of in vitro half-life approach and nonspecific binding to microsomes. *Drug Metab Dispos* **1999**; 27:1350–9.
21. Hargrove TY, Wawrzak Z, Alexander PW, et al. Complexes of *Trypanosoma cruzi* sterol 14 α -demethylase (CYP51) with two pyridine-based drug candidates for Chagas disease: Structural basis for pathogen selectivity. *J Biol Chem* **2013**; 288:31602–15.
22. Villalta F, Kierszenbaum F. Immunization against a challenge with insect vector, metacyclic forms of *Trypanosoma cruzi* simulating a natural infection. *Am J Trop Med Hyg* **1983**; 32:273–6.
23. Nakayama H, Loiseau PM, Bories C, et al. Efficacy of orally administered 2-substituted quinolines in experimental murine cutaneous and visceral leishmaniases. *Antimicrob Agents Chemother* **2005**; 49:4950–6.
24. Lepesheva GI, Hargrove TY, Anderson S, et al. Structural insights into inhibition of sterol 14 α -demethylase in the human pathogen *Trypanosoma cruzi*. *J Biol Chem* **2010**; 285:25582–90.
25. Lepesheva GI. Design or screening of drugs for the treatment of Chagas disease: what shows the most promise? *Expert Opin Drug Discov* **2013**; 8:1479–89.
26. Hargrove TY, Wawrzak Z, Liu J, Waterman MR, Nes WD, Lepesheva GI. Structural complex of sterol 14 α -demethylase (CYP51) with 14 α -methyl-enecyclopropyl- Δ 7–24, 25-dihydrolanosterol. *J Lipid Res* **2012**; 53:311–20.
27. Lepesheva GI, Nes WD, Zhou W, Hill GC, Waterman MR. CYP51 from *Trypanosoma brucei* is obtusifoliol-specific. *Biochemistry* **2004**; 43:10789–99.
28. Cherkasova TS, Hargrove TY, Vanrell MC, et al. Sequence variation in CYP51A from the Y strain of *Trypanosoma cruzi* alters its sensitivity to inhibition. *FEBS Lett* **2014**; 588:3878–85.
29. Heeres J, Meerpoel L, Lewi P. Conazoles. *Molecules* **2010**; 15:4129–88.
30. Richardson K, Cooper K, Marriott MS, Tarbit MH, Troke PF, Whittle PJ. Discovery of fluconazole, a novel antifungal agent. *Rev Infect Dis* **1990**; 12:S267–271.
31. Hargrove TY, Kim K, de Nazaré Correia Soeiro M, et al. CYP51 structures and structure-based development of novel, pathogen-specific inhibitory scaffolds. *Int J Parasitol Drugs Drug Resist* **2012**; 2:178–86.
32. Dalvie DK, Kalgutkar AS, Khojasteh-Bakht SC, Obach RS, O'Donnell JP. Biotransformation reactions of five-membered aromatic heterocyclic rings. *Chem Res Toxicol* **2002**; 15:269–99.
33. Troke PF AR, Pye GW, Richardson K. Fluconazole and other azoles: translation of in vitro activity to in vivo and clinical efficacy. *Rev Infect Dis* **1990**; 12(suppl 3):S276–80.
34. Brüggemann RJM, Alffenaar J-WC, Blijlevens NMA, et al. Clinical relevance of the pharmacokinetic interactions of azole antifungal drugs with other coadministered agents. *Clin Infect Dis* **2009**; 48:1441–58.
35. Lewis MD, Fortes Francisco A, Taylor MC, et al. Bioluminescence imaging of chronic *Trypanosoma cruzi* infections reveals tissue-specific parasite dynamics and heart disease in the absence of locally persistent infection. *Cell Microbiol* **2014**; 16:1285–300.
36. Roberts CW, McLeod R, Rice DW, Ginger M, Chance ML, Goad LJ. Fatty acid and sterol metabolism: potential antimicrobial targets in apicomplexan and trypanosomatid parasitic protozoa. *Mol Biochem Parasitol* **2003**; 126:129–42.
37. Goad L, Holz GJ, Beach D. Sterols of *Leishmania* species. Implications for biosynthesis. *Mol Biochem Parasitol* **1984**; 2:61–170.
38. Paniz Mondolfi AE, Stavropoulos C, Gelanew T, et al. Successful treatment of Old World cutaneous leishmaniasis caused by *Leishmania infantum* with posaconazole. *Antimicrob Agents Chemother* **2011**; 55:1774–6.
39. Baroni A, Aiello FS, Vozza A, et al. Cutaneous leishmaniasis treated with itraconazole. *Dermatol Ther* **2009**; 22:S27–9.
40. Akuffo H, Dietz M, Teklemariam S, Tadesse T, Amare G, Berhan T. The use of itraconazole in the treatment of leishmaniasis caused by *Leishmania aethiopicum*. *Trans R Soc Trop Med Hyg* **1990**; 84:532–4.
41. Dedet J, Jamet P, Esterre P, Ghipponi P, Genin C, Lalande G. Failure to cure *Leishmania braziliensis* guyanensis cutaneous leishmaniasis with oral ketoconazole. *Trans R Soc Trop Med Hyg* **1986**; 80:176.
42. Rangel H, Dagger F, Hernandez A, Liendo A, Urbina JA. Naturally azole-resistant *Leishmania braziliensis* promastigotes are rendered susceptible in the presence of terbinafine: comparative study with azole-susceptible *Leishmania mexicana* promastigotes. *Antimicrob Agents Chemother* **1996**; 40:2785–91.

43. Navin TR, Arana BA, Arana FE, Berman JD, Chajón JF. Placebo-controlled clinical trial of sodium stibogluconate (pentostam) versus ketoconazole for treating cutaneous leishmaniasis in Guatemala. *J Infect Dis* **1992**; 165:528–34.
44. Berman JD. Human leishmaniasis: clinical, diagnostic, and chemotherapeutic developments in the last 10 years. *Clin Infect Dis* **1997**; 24: 684–703.
45. Aperis G, Mylonakis E. Newer triazole antifungal agents: pharmacology, spectrum, clinical efficacy and limitations. *Expert Opin Investig Drugs* **2006**; 15:579–602.
46. Vanden Bossche H. Mode of action of pyridine, pyrimidine and azole antifungals. In: Berg DaP M ed. *Sterol Biosynthesis Inhibitors*. Vol. 79–119. Chichester: Ellis Horwood, **1988**:79–119.
47. Gigante F, Kaiser M, Brun R, Gilbert IH. Design and preparation of sterol mimetics as potential antiparasitics. *Bioorg Med Chem* **2010**; 18: 7291–301.
48. Van den Bossche H, Willemsens G, Cools W, Cornelissen F, Lauwers WF, van Cutsem JM. In vitro and in vivo effects of the antimycotic drug ketoconazole on sterol synthesis. *Antimicrob Agents Chemother* **1980**; 17:922–8.
49. Lepesheva GI, Zaitseva NG, Nes WD, et al. CYP51 from *Trypanosoma cruzi*: a phyla-specific residue in the B' helix defines substrate preferences of sterol 14 α -demethylase. *J Biol Chem* **2006**; 281:3577–85.
50. Bustamante JM, Craft JM, Crowe BD, Ketchie SA, Tarleton RL. New, combined, and reduced dosing treatment protocols cure *Trypanosoma cruzi* infection in mice. *J Infect Dis* **2014**; 209:150–62.